

ENHANCEMENT OF TIMS IMAGES FOR PHOTOINTERPRETATION

A.R. Gillespie

Geology Group
Jet Propulsion Laboratory
California Institute of Technology
Pasadena, California 91109

ABSTRACT

TIMS images consist of six channels of data acquired in bands between 8 and 12 μm ; thus they contain information about both temperature and emittance. Scene temperatures are controlled by the reflectivity of the surface, but also by its geometry with respect to the sun, time of day, and other factors unrelated to composition. Emittance is dependent upon composition alone. Thus the photointerpreter may wish to enhance emittance information selectively. Because thermal emittances in real scenes vary but little, image data tend to be highly correlated among channels. Special image processing is required to make this information available for the photointerpreter. Processing includes noise removal, construction of model emittance images, and construction of false-color pictures enhanced by decorrelation techniques.

INTRODUCTION

Thermal infrared radiance measurements historically have been used to estimate temperatures of surfaces. Thermal infrared images have generally been used the same way. Thermal radiance is related to the temperature of a surface through Planck's Law and a proportionality factor known as the thermal emissivity or emittance. The temperature is a function of a number of factors. Among these are: reflectivity in visible and near-infrared wavelengths, thermal inertia of the material composing the surface, the geometry of the surface with respect to the sun, the time of day, and various characteristics of the atmosphere. Some of these factors - the reflectivity and thermal inertia - are intrinsic properties of the composition of the exposed material. Other factors are properties of the surface itself. Still others have nothing to do with the surface, but depend on the weather, time of day, and so forth. Thus radiance images convey much information, but not necessarily in a simple way.

Thermal emittance of the earth's surface, on the other hand, is controlled largely by the composition of the surface material, by the texture of the surface, and by the local topography, independent of lighting conditions, weather, or time of day. Furthermore, emittance varies with wavelength in a way that is

distinctive for many silicate and other rock-forming minerals [Lyon, 1965]. Thus emittance spectra are a useful aid in lithologic mapping and other geologic studies.

TIMS images are multispectral; they consist of six channels of radiance data acquired in bands between 8 and 12 μm [Palluconi and Meeks, 1985]. Thus they contain information about both the temperature of a surface, and also its emittance spectrum.

The photointerpreter has at his disposal a wealth of information in TIMS images. If he is interested in surface composition, he may choose to enhance emittance information selectively. Because thermal emittances in real scenes vary but little, image data tend to be highly correlated among channels. Special image processing is required to make this information available for the photointerpreter. Processing includes noise removal, calculation of model emittance images, and construction of false-color pictures enhanced by decorrelation techniques.

ENHANCEMENTS

Noise Removal

TIMS data contain noise from a number of sources. In addition to random detector noise, which has an NE Δ T of $\sim 0.2^\circ$ at 300 K [Palluconi and Meeks, 1985], there is found both low- and high-frequency striping, microphonic interference and a signal-dependent bit error in one preamplifier (Ch. 6). Some of these components may be removed by the appropriate image-processing technique, but each requires a different approach.

Random Noise... Random detector noise is intrinsically part of the image data. The dynamic range is chosen such that the noise level is generally ± 1 DN. Pixels having DN that are radically different than neighboring values can be recognized and removed with a variety of techniques, most notably median filtering. Approaches such as this will also remove "deviant" or unusual signal, however. In general, the amplitude of random detector noise in TIMS is too low to warrant efforts to suppress it.

Bit Errors... Unlike the low-amplitude random noise, bit errors are obvious defects in the TIMS data. They appear to occur when there are strong and rapid changes in the scene radiance; thus the bit errors will often be encountered on one side of a sharp high-contrast feature in a scene. They are generally removed by bilinear interpolation, in algorithms that compare local to neighboring DN values. Local values that exceed the mean DN of the neighboring pixels by more than a settable threshold are replaced by the mean DN itself. Median filters also are effective at suppressing this type of noise.

Bit errors seem to occur infrequently, but their tendency to be grouped along interesting image features (edges) is disruptive to

photointerpretation. Therefore their removal is usually helpful.

Low-Frequency Striping... TIMS data frequently contain a low-amplitude, low-frequency striping or banding that is attributed to changes in detector sensitivity. Although the striping is so subtle (<10% of the encoded radiance) that it may be difficult to see in images made from the radiance data, it tends to be poorly correlated among channels. Therefore this striping is "colored;" it masquerades as scene emittance changes. In fact, the amplitude of this source of noise in emittances may be so high that it is the greatest source of variance in the emittance images. False-color images made from calculated emittance values may be dominated by the low-frequency striping. In these pictures the low-frequency striping looks like varicolored horizontal bands or bars about 200 image lines high. Because emittance is often the parameter of greatest interest in TIMS data, this striping is a serious problem. For photointerpretation, striping removal is desirable. For calculating meaningful emittance data, removal is necessary.

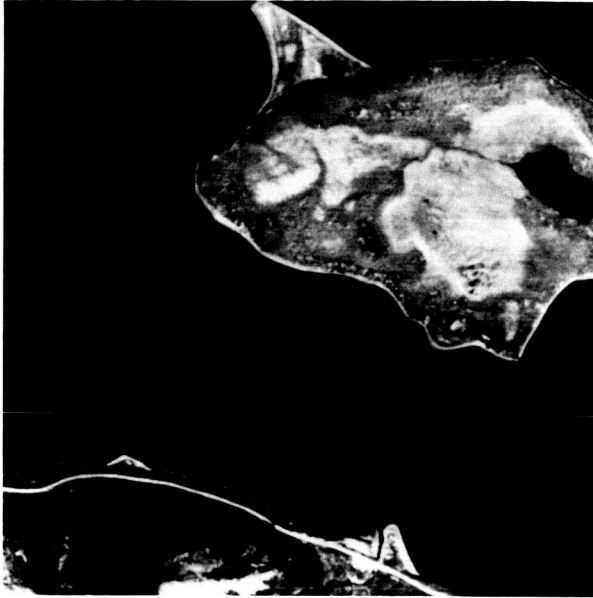
Fortunately, TIMS scans a hot and a cold blackbody of measured kinetic temperatures once per image line. Since the detector response to the thermal photon flux is linear [Palluconi and Meeks, 1985], this information is adequate to calibrate the detectors line by line. The procedure is simple: The photon flux from the reference blackbodies for each TIMS channel is calculated using the measured temperatures, the spectral sensitivity of the detectors and filters, and Planck's Law. From this information the linear equation relating the DN values reported for the blackbodies to the calculated fluxes is found. This will vary from scan line to scan line. Then the photon fluxes for the image pixels are found, using the reported DN values and the linear coefficients found from the calibration data.

Use of the TIMS on-board calibration data as described above is effective in suppressing the low-frequency striping due to detector sensitivity changes. In enhanced pictures the banding will no longer be visible. But some extra precautions are necessary in processing to avoid *introducing* additional high-frequency striping during banding suppression. The problem arises because, like the image data, the calibration data are contaminated by microphonic noise and occasional dropped bits. Obviously, if the data used to calibrate the image are themselves in error, striping removal will be ineffectual or worse. However, because the detector sensitivity changes slowly, any high-frequency fluctuations in the calibration data must be caused by noise. Drop-outs may be removed from the calibration data by median filtering; then high-frequency microphonic noise may be removed by low-pass filtering in either the spatial or frequency domain. These precautions should always be taken.

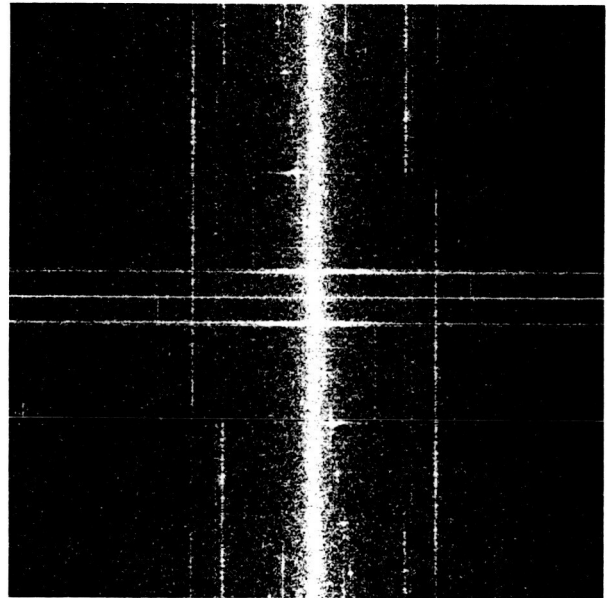
High-Frequency Striping... A major source of high-frequency striping in TIMS data is microphonic vibration of the detector, which sits on a long stem in its dewar. In one TIMS image of Newfoundland, microphonic noise was oblique to the scan lines and

A.R. Gillespie: Enhancement of TIMS data...

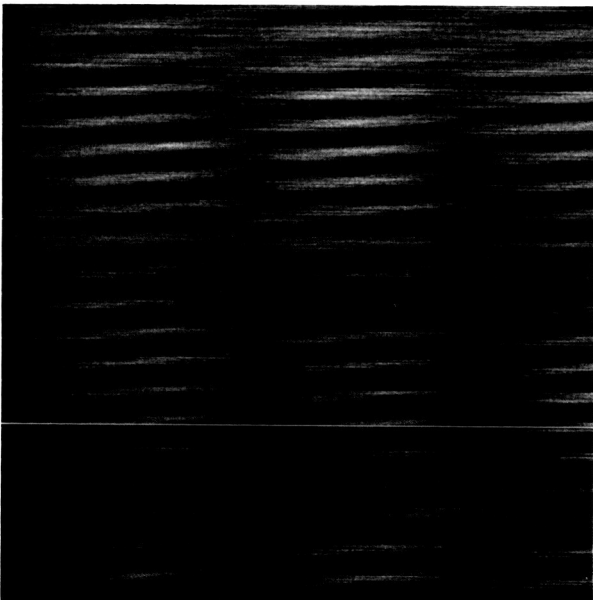
had wavelengths of 200 samples and 25 lines per cycle (Figure 1). The exact frequencies are variable, even if the image is acquired at the same scan rate. Obviously, the angle of the striping and its frequency in the scan direction vary with the scan speed selected during data acquisition by the technicians operating TIMS.



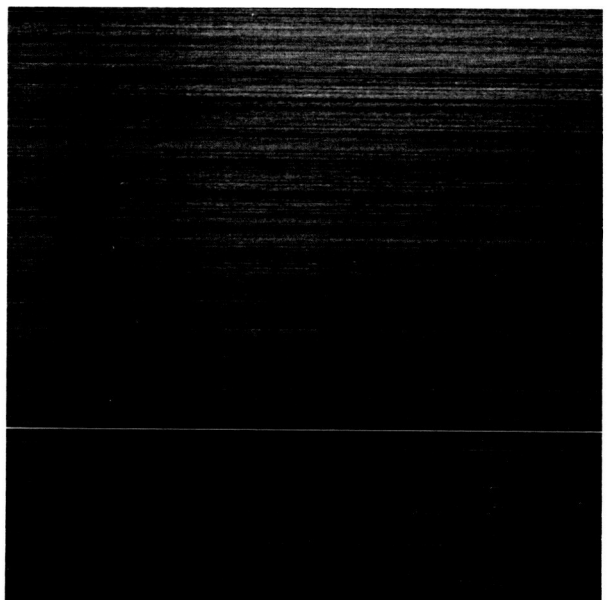
a



b



c



d

Figure 1. A TIMS image of Newfoundland, showing noise. (a) Radiance image. (b) Two-dimensional Fourier transform of an image subscene. The modulus is displayed as black (zero) to white (high). Frequencies vary from zero (origin, at center) to 0.5 cycles/pixel (edge). Horizontal axis displays frequencies in the scan direction. (c) Microphonic noise removed from the image. (d) residual striping in image after microphonic noise was removed.

Figure 1 shows (a) a TIMS image of Newfoundland, (b) a two-dimensional Fourier transform of the image data, (c) the microphonic noise found in the image, and (d) residual horizontal striping that remained after the microphonic noise was removed. Very little microphonic noise is seen in the radiance image. However, the Fourier transform shows large bands and spikes that correspond to the noise. Additionally, the transform has large amplitudes on the axes. These occur if there are radiance gradients across the image, because of the periodic nature of the transform. Finally, this particular image was geometrically corrected before it was transformed, to compensate for panorama foreshortening. This has the effect in the transform of spreading out noise spikes in the scan (horizontal) direction.

Most of the image data are concentrated in a continuum near the origin of the transform. The obvious noise in Figure 1d has frequencies that plot near the continuum also, a little more than 1 pixel away in the scan direction and ~ 20 pixels away in the line direction (1st and 3rd quadrants). The microphonic noise is not spectrally pure, and its dominant frequencies are not necessarily simple integer factors lower than the Nyquist frequency. Because of these effects, the dominant noise spike is distributed in a cross, orthogonal to the coordinate system. In this instance, scan-direction smearing by the geometric corrections discussed above appears to have been significant.

The noise images shown in Figures 1c,d were isolated using the techniques described below. The source of the residual striping is uncertain. Some of it may result because of changes in detector sensitivity during the interval between measurement of the internal reference and measurement of the scene. High-frequency striping in TIMS data is variable in amplitude; it is not always a dominant component of the image. However, as with the banding due to changing detector sensitivity, even subtle striping is exaggerated by processing the image to extract emittance data, or in constructing radiance ratio images. Below, ratioed radiance data from a relatively noise-free TIMS image of Death Valley, California, are used to illustrate high-frequency striping removal by filtering in the frequency (Fourier) domain.

Figure 2 shows the TIMS image of Trail Canyon Fan, across Death Valley from Monument Headquarters at Furnace Creek. An enhanced false-color picture of this image is in Kahle and Goetz [1983] or in Gillespie et al. [1984]. Figure 2a is the ratio picture of TIMS channels 5/6, before noise removal. The microphonic noise is nearly diagonal in this picture, with a wavelength of ~ 50 pixels. Additionally, subhorizontal high-frequency striping is evident. Finally, bit errors (dark in Channel 6) appear as bright spots, especially evident on the west sides of the dark regions on the valley floor. The bit errors were identified and removed using the approach discussed above, before transforming the image to the Fourier domain. Figure 4b shows the Fourier transform of the ratio image. The obvious microphonic noise is confined to two horizontal bars near the horizontal axis, as for the Newfoundland image, and for the same reasons.

A.R. Gillespie: Enhancement of TIMS data...

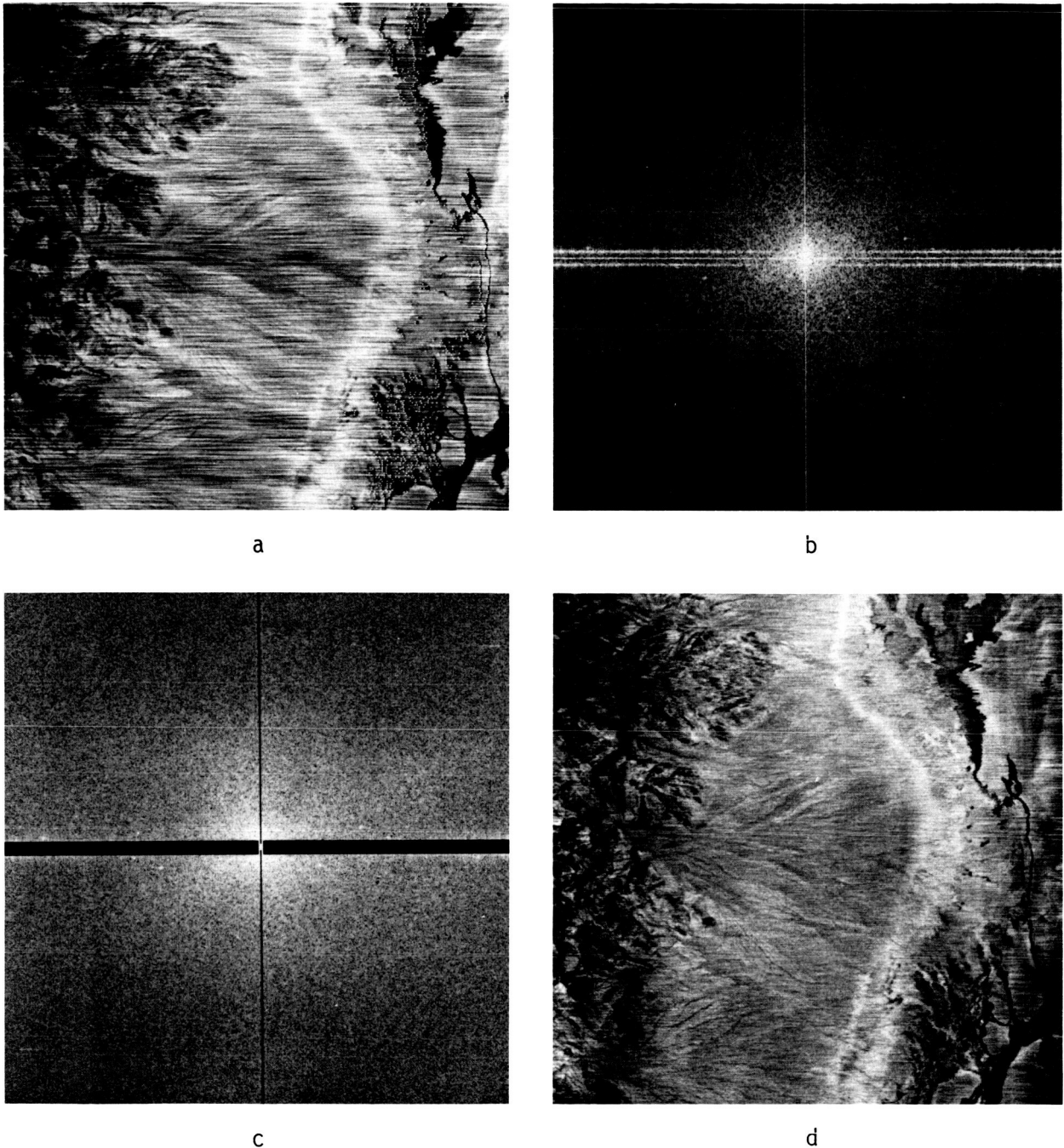


Figure 2. TIMS image of Death Valley, California. (a) Ratio picture, Channels 5/6, showing microphonic noise. (b) Fourier transform. (c) Fourier transform with noise masked out. (d) Ratio image with microphonic noise removed.

Filtering in the Fourier domain is readily accomplished by multiplying the transform by a mask (the filter) that passes or rejects data. It is not necessary that the filter be a binary function, but for this example it was. Figure 1c shows the filtered transform of Figure 1b. The filter multiplied by zero those image components that plot on the vertical axis or near the

horizontal axis (except very near the origin). The filtered image was then reconstructed by performing a Fourier transformation on the filtered transform (inverse transformation). The filtered ratio picture is shown in Figure 1d. cursory inspection shows that most of the microphonic noise has been suppressed.

Detailed inspection of the filtered image of Figure 1d reveals a number of directional artifacts that appear as an oriented fabric [Gillespie, 1980]. These undesired artifacts are consequences of removing too much power from the image near the zero-frequency axes. The fabric can be suppressed using a more complicated filter that passes data in a narrow horizontal bar within the suppressed bar of Figure 1c. These results are not shown here.

Filtering in the Fourier domain is a conceptually simple approach to removing noise in digital images that has been successfully used on a wide range of projects [e.g., Rindfleisch et al., 1971]. There are drawbacks, however, for the user of small computers. The transform is computationally expensive; the fast Fourier transform (FFT) requires the period of the image chip to be a power of two. The TIMS data are not. There are ways to solve this problem: the image may be "padded" with gray data to widen it; it may be truncated to make it smaller; or the FFT need not be used to perform the transformation.

Another approach is to filter the image in the spatial domain (as acquired), by convolution. In general, two-dimensional convolution is an expensive procedure, but because most of the noise in the TIMS data is subparallel with either the scan or the flight axis only a one-dimensional filter is required. The weights in the filter kernel are found from the 1-D transform of the frequency-domain filter discussed above. These may be calculated analytically, for simple filters [e.g., Castleman, 1979].

The general equation for a 1-D spatial-domain filter kernel that has the same effect as the binary filter discussed above is given by:

$$h(x) = \delta(x) - 2\Delta s \frac{\sin(\pi \Delta s x)}{\pi \Delta s x} \cos(2\pi s_0 x) \quad (1)$$

where h is the filter kernel, x is the kernel sample value in the scan or flight direction, as appropriate, and s is the frequency in the transform. The filter kernel is centered at $x = 0$. The Kronecker delta function $\delta(x)$ is an all-pass filter:

$$\left[\begin{array}{l} \delta(x) = 1 : x = 0 \\ \delta(x) = 0 : x \neq 0 \end{array} \right] \quad (2)$$

Kernel $h(x)$ is a high-pass filter. The frequencies that are not passed by $h(x)$ are specified by the right-hand terms of equation

1: s_0 is the central frequency to be suppressed, and Δs is the range of frequencies centered on s_0 to be suppressed. The cosine term is the transform of the impulse pair at s_0 in the frequency domain. The sinc function is the transform of a rectangular pulse of width Δs (in the frequency domain).

Now for the discrete transform of an image of NS samples, the frequency interval Δs corresponding to a sample interval Δx in the transform is given by:

$$\Delta s = \frac{\Delta x}{NS/2} \cdot 0.5 = \frac{\Delta x}{NS} \quad (3)$$

The factor of 0.5 in Equation 3 is the Nyquist frequency. Thus, if we suppress the smallest range of frequencies possible in the discrete transform of a 1024-sample image ($\Delta x = 1$), $\Delta s = 1/1024$ and

$$h(x) = \delta(x) - \frac{\text{sinc}(\pi x/1024)}{512} \cos(2\pi s_0 x) \quad (4)$$

Weights for the convolution filter may be found from equation 4, or a similar expression if other filter characteristics are desired.

Convolution filtering has two noteworthy drawbacks: first, the filters will "feel" the edge of data when they are half their width from an edge. This results in a bright or dark artifactual band down the sides of the image (horizontal filter) or along the top and bottom (vertical filter). This artifact can be reduced in severity by reflecting the image about its limits and filtering the reflected data, together with the actual image, but additional computational cost is incurred.

A second problem is that if it is necessary to suppress a narrow band of frequencies (Δs is small, as in equation 4), the number of weights required is large. If too few filter weights are used the filter will not pass the data accurately; it also may "ring," or sense high-contrast features in the image when it is centered some distance away. Ringing caused by a poorly designed filter can be quite annoying to the photointerpreter (Figure 3). It can be reduced by using a frequency-domain filter with softer edges than the binary mask; e.g., weights described by a Gaussian function. In this case, the right-hand terms in Equation 1 must be multiplied by the transform of the new function (in this example, another Gaussian function) instead of the sinc function.

Although this practice was not followed in producing the examples used above, it is important to filter the image before panorama correction. In this way, the noise is not dispersed throughout the spectrum, and the filter can be designed to remove less signal.

ORIGINAL PAGE IS
OF POOR QUALITY

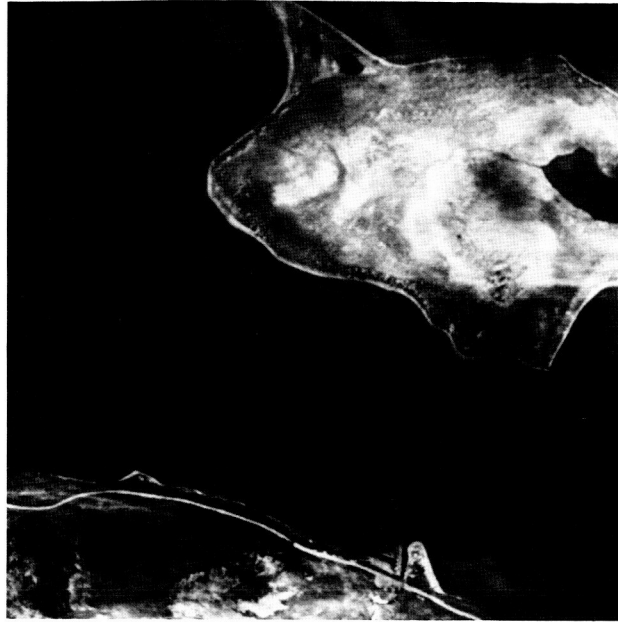


Figure 3. The TIMS image of Newfoundland (Fig. 1a), filtered by convolution with a 1-D filter kernel that induced excessive "ringing" off hard edges.

Analysis: Model Emittance Calculation

Once the noise has been removed from the TIMS data, and the images have been calibrated in units of photon flux, they are ready for analysis. In geological applications, the emittance (ϵ) information imbedded in the radiance data is of great significance, because it is related to the composition of the imaged surface, especially for silicate rocks. On the other hand, the temperature varies with topography, and throughout the day. It is only indirectly related to the surface composition. Thus it is desirable to separate temperature and emittance information.

Unfortunately, with six channels of data and seven unknowns (six emittance values and the temperature) the problem is underdetermined. We must make an assumption in order to calculate anything at all. The assumption generally made is that the emittance ϵ_6 channel 6 (with a bandpass centered at $\sim 11 \mu\text{m}$) is known. Its value ϵ' is generally taken to be about 0.93 (emittance ranges from 0 to 1), thought to be typical for a wide range of silicate minerals. However, this assumption is generally not true for mafic and ultramafic silicate rocks, and this must be remembered in interpreting emittance data calculated this way. In general, it is useful to identify emittances ϵ' calculated from thermal IR scanners as "model emittances," so that the basic assumption is not overlooked.

The temperature T at which the surface is radiating is approximated using Planck's Law, for the photon flux or radiance

R in Channel 6:

$$T_6 = \frac{c_2}{\lambda_6} \left[\ln \left[\frac{\epsilon'_6 c}{R_6 \lambda_6^4} + 1 \right] \right]^{-1} \quad (5)$$

where λ_6 is the wavelength for channel 6. Strictly, there is no single value of λ_6 , because the bandpass for channel 6 is 11.2-12.2 μm , so in order to calculate R_6 Planck's Law must be integrated over λ . Equation 5 would be accordingly more complicated, but for the purposes of this discussion it is simplified by assuming that the bandpass is quite narrow and there does exist a single value for λ_6 .

Parameter $c_2 = hc/k$ in equation 5 is a constant, and ϵ'_6 is the emittance assumed for channel 6. The parameter c is the speed of light; h is Planck's constant; and k is Boltzmann's constant. Because the TIMS detectors respond to the photon flux, rather than the energy [Palluconi and Meeks, 1985], the right side of equation 5 has been divided by a factor of hc/λ (the energy for a photon of wavelength λ).

Once T_6 is estimated, model blackbody values of R'_i can be calculated for channels 1-5, according to:

$$R'_i(T_6) = \frac{c}{\lambda_i^4} \frac{1}{\{\exp[c_2/(\lambda_i T_6)] - 1\}} \quad (6)$$

Emittance ϵ is the proportionality constant between observed radiance and the ideal radiance from a blackbody at the same kinetic temperature. Therefore, we may calculate model emittances ϵ'_i according to

$$\epsilon'_i = \epsilon'_6 \frac{R_6}{R'_i} \quad (7)$$

Images made of model emittance data show little topography or temporal heating patterns; they show largely compositional information. Pictures of such emittance data for Death Valley are given in Kahle and Walker [1984].

As mentioned above, the assumption that $\epsilon'_6 = 0.93$ is not valid for mafic rocks; measured values are lower. Thus emittance data for some channels of TIMS data may exceed unity over ultramafic and mafic rocks. What has happened is that the reststrahlen band (Si - O vibration) has shifted to longer wavelengths in mafic minerals. Consequently, for mafic minerals a better assumption would be that $\epsilon'_i = 0.93$ [e.g., Lyon, 1965]. It is computationally simple to find the channel for which the apparent T_i is maximum. If we assume a value for the maximum ϵ , and not

restrict the channel for which it is found, we can calculate reasonable values of ϵ' regardless of the type of silicate rock in the scene.

Finally, it may be useful to estimate the wavelength of the reststrahlen band and report that information as an image. Gillespie and Abbott [1984] showed that this parameter is sensitive to silicate mineralogy in a range of TIMS images. They estimated the central wavelength of the reststrahlen band by fitting a Gaussian function to the emittance data. Other reported parameters were the width of the reststrahlen band (standard deviation) and the intensity (difference between minimum and maximum emittance values).

Decorrelation Stretching

Commonly, it is desired to display false-color pictures made from three selected channels of TIMS data. It is easier to interpret these data if some topographic (temperature) data is left in the pictures. Also, if noise removal is incomplete, or for very noisy data, the emittance data will be heavily striped.

Soha and Schwartz [1978] devised a technique to exaggerate the highly correlated emittance information, while retaining some of the temperature information. They called this method the "decorrelation stretch" because it involved calculating statistically independent or orthogonal images in which the covariance was zero. This was done by principal-component analysis.

Early efforts to use principal-component images as red-green-blue (RGB) components of false-color pictures were successful in producing brightly colored pictures, but these were hard to interpret in terms of physical processes in the scene. Soha and Schwartz intended to produce a false-color picture in which there was little distortion of hue, but in which color saturation or chroma was exaggerated and the intensity or lightness was suppressed. This they did by equalizing the variance in the principal-component images, and then applying the inverse transformation to recreate the images in the original RGB domain. False-color pictures made from "decorrelation-stretched" images were colorful, but could easily be related to the original images or to spectral data describing the scene. An example of a "decorrelated" false-color picture may be found in Kahle and Rowan [1980]. A thorough discussion of the method may be found in Gillespie et al. [1986].

SUMMARY

TIMS data can be used both for photointerpretation and scene analysis, but careful processing is in general necessary before they may be used. This processing involves image calibration to suppress effects due to detector sensitivity changes, and filtering to remove microphonic and other high-frequency striping

noise. Additionally, it may be necessary to identify bit errors in the image and remove them by interpolation. Once the image is free of artifacts, additional processing is necessary to separate emittance and temperature information. This is desirable because emittance information describes the composition of the imaged scene, especially if it contains silicate minerals. Wavelengths of reststrahlen bands may be estimated from emittance data by curve-fitting techniques. This information is related to rock type. Alternatively, images may be prepared for photointerpretation by "decorrelating" them before contrast-stretching and construction of false-color pictures.

ACKNOWLEDGEMENTS

NSTL personnel, particularly G. Meeks, have been unstinting in their support, operation, and improvement of TIMS. The research described in this paper was carried out at the Jet Propulsion Laboratory of the California Institute of Technology and sponsored by the Land Processes Branch of the National Aeronautics and Space Administration.

REFERENCES CITED

- Castleman, K., 1979, Digital Image Processing, Prentice Hall, New York, pp 139-225.
- Gillespie, A.R., 1980, Digital techniques of image enhancement, in Siegal, B.S., and A.R. Gillespie, eds., Remote Sensing in Geology, Wiley, New York, pp 216-219.
- Gillespie, A.R. and E.A. Abbott, 1984, Mapping Compositional Differences in Silicate Rocks with Six-Channel Thermal Images, Proc. 9th Canadian Symposium on Remote Sensing, St. Johns, Newfoundland, pp 327-336.
- Gillespie, A.R., A.B. Kahle and F.D. Palluconi, 1984, Mapping alluvial fans in Death Valley using multichannel thermal infrared images, *Geophys. Res. Lett.* 11, 1153-1156.
- Gillespie, A.R., A.B. Kahle and R.E. Walker, 1986, Color enhancement of highly correlated images: I. Decorrelation and HSI stretches, *Remote Sensing of Environment*, in press.
- Kahle, A.B. and L.C. Rowan, 1980, Evaluation of Multispectral Middle Infrared Aircraft Images for Lithologic Mapping in East Tintic Mountains, Utah, *Geol.* 8, 234-239.
- Kahle, A.B. and R.E. Walker, 1984, Calculation of Emissivity and Thermal Inertia at Death Valley, California, from TIMS Data, Proc. 9th Canadian Symposium on Remote Sensing, St. Johns, Newfoundland, pp 337-346.
- Kahle, A.B. and A.F.H. Goetz, 1983, Mineralogic Information From a New Airborne Thermal Multispectral Scanner, *Science*, 222, 24-27.

A.R. Gillespie: Enhancement of TIMS data...

Lyon, R.J.P., 1965, Analysis of Rocks by Spectral Infrared Emission (8 to 25 Microns), *Econ. Geol.*, 60, 715-736.

Palluconi, F.D., and G.R. Meeks, 1985, Thermal Infrared Multispectral Scanner (TIMS): An investigator's guide to TIMS data, JPL Publication 85-32, Jet Propulsion Laboratory, Calif. Inst. Technology, Pasadena, CA, 22 pp.

Soha, J.M. and A.A. Schwartz, 1978, Multispectral Histogram Normalization Contrast Enhancement, *Proc. 5th Canadian Symposium on Remote Sensing*, Victoria, B.C., pp 86-93.

Rindfleisch, T.C., J.A. Dunne, H.J. Frieden, W.D. Stromberg, R.M. Ruiz, 1971, Digital processing of the Mariner 6 and 7 pictures, *Jour. Geophys. Res.*, 76, 394-417.

* * * * *